Journal of Applied Electrochemistry **33**: 1125–1135, 2003.

The role of defects, or active states, in surface electrochemistry with particular reference to gold in neutral solution

L.D. BURKE, A.M. O'CONNELL and A.P. O'MULLANE
Chemistry Department, University College Cork, Cork, Ireland

Received 9 September 2002; accepted in revised form 13 June 2003

Key words: active states, electrocatalysis, gold, hydrous oxides, neutral solution

Abstract

Metastable, active, or nonequilibrium states due to the presence of abnormal structures and various types of defects are well known in metallurgy. The role of such states at gold surfaces in neutral aqueous media (an important electrode system in the microsensor area) was explored using cyclic voltammetry. It was demonstrated that, as postulated in earlier work from this laboratory, there is a close relationship between premonolayer oxidation, multilayer hydrous oxide reduction and electrocatalytic behaviour in the case of this and other metal electrode systems. Some of the most active, and therefore most important, entities at surfaces (e.g., metal adatoms) are not readily imageable or detectable by high resolution surface microscopy techniques. Cyclic voltammetry, however, provides significant, though not highly specific, information about such species. The main conclusion is that further practical and theoretical work on active states of metal surfaces is highly desirable as their behaviour is not simple and is of major importance in many electrocatalytic processes.

1. Introduction

Little attention has yet been given in surface electrochemistry to the detail that solid metals can trap and store energy and exist in metastable or nonequilibrium states. Metal atoms at defect sites are often protruding species which are thermodynamically active as they have a low lattice stabilization energy; also, atoms present in microcluster states are unusually active due to quantum confinement effects. Such states are well known for bulk metals in metallurgy [1, 2] and for thin metal films in the microelectronics fabrication industry [3, 4]. Generally, the equilibrium state of a metal is highly ordered, with virtually all lattice points occupied. Metastable states and energy storage are associated with lattice defects, for example, the metal may be amorphous or poorly crystallized or contain an unusually high density of extended defects (dislocations) [2]. The metastable state is difficult to investigate as (i) it is almost infinitely variable, the type and density of defects, or the degree of noncrystallinity, being not easily controlled, and (ii) since such states are intrinsically unstable they are prone to alter easily with time or treatment. However, the behaviour of metals in such states is of increasing importance as may be judged by the market value of metastable metals which was quoted in 1991 at about US $0.3 billion per annum [1].

It is widely accepted in surface and interfacial science that defects, which are the essence of energy storage in metals, are common at real surfaces. According to Adamson [5] 'not all atoms on the surface are equivalent in nature; those present at ragged asperities are much more energy-rich than those with a normal number of nearest neighbours and possess a higher than average surface energy and surface mobility'. Attempts to circumvent the surface defect problem by the use of single crystal plane surfaces seem to be frustrated by the fact that these model systems usually contain plenty of imperfections [6, 7]. More importantly, from a surface catalysis viewpoint, it has been pointed out that roughness, or disorder, is a prime requirement for high catalytic activity [8]; this may be regarded as a restatement of Taylor's active site theory of heterogeneous catalysis [9].

Metal activation and its effect on surface electrochemistry has been a topic of research in this laboratory for several years. The type of activation in question here is energetic (or thermodynamic, $\mu_{\mathrm{Me}} \gg \mu^{\circ}_{\mathrm{Me}}$) rather than kinetic, and in most cases the high energy state was achieved by doing work on the metal sample under investigation. Activation techniques used earlier include potential cycling + abrasion (for Pt [10]), thermal pretreatment (for Pt and Au [11–13]), cathodization or hydrogen embrittlement (for Au, Pt and Cu [14, 15]) and repeated multilayer oxide growth and reduction (for Pd [16]). The mechanism of energy storage involves extensive defect generation; this may entail an increase in surface area but, much more importantly, it involves a severe reduction in the lattice stabilization energy of surface metal atoms. These more active atoms tend to undergo oxidation at unusually low potentials; such a process, referred to as premonolayer or underpotential oxidation, was investigated extensively recently by Doblhofer and coworkers [17–20] in the case of silver in base; its relevance to the electrocatalytic behaviour of gold in aqueous acid and base was reviewed recently [21] and an overview of the active state behaviour of gold electrode surfaces has just been published [22].

The present work is concerned mainly with the behaviour of gold in neutral aqueous media; this is an important area with regard to microsensors, especially in connection with the analysis of biological samples [23–25]. Premonolayer oxidation, multilayer oxide growth and some electrocatalytic responses were investigated using electrochemical techniques and the implications of the results are discussed. Some data for gold in acid are also included to illustrate the general application of the ideas outlined here.

2. Experimental details

The type of equipment used in this work was described earlier [14]. The working and counter electrodes were approximately of the same size; they consisted of lengths of gold wire (1.0 mm dia., ~0.8 cm^2 exposed area, Johnson Matthey, Puratronic grade) sealed directly into soda glass. Prior to use the surface of the working electrode was subjected to mild abrasion with fine grade emery paper followed by washing with triply distilled water. The main exception in this respect was the thermally pretreated electrode where the response shown, Figure 2(b), was recorded directly after heating. The potential of the gold electrode was generally cycled (0.0–1.8 V, 50 mV s^{-1}) initially to ensure that the conventional response, Figure 1(a), was observed.

Potentials were recorded with respect to a hydrogen reference electrode in the same solution. Solutions were made up using Analar grade chemicals and triply distilled water and were purged with oxygen-free nitrogen before use. The phosphate buffer solution contained 0.025 mol dm^{-3} KH_2PO_4 and 0.025 mol dm^{-3} Na_2HPO_4. The cyclic voltammograms reported are direct recorder plots, reproduced with the aid of a scanner plus a computer.

3. Results

3.1. *Effect of cathodic polarization*

A typical cyclic voltammogram for an untreated gold wire electrode in aqueous neutral solution is shown in Figure 1(a). The positive sweep was featureless until the onset at about 1.30 V of monolayer oxide film formation. In the subsequent negative sweep this monolayer oxide film was reduced over the potential range 1.20–1.00 V, the hysteresis between the oxide formation and reduction response being quite evident. This was followed by an extended double layer region to the end of the sweep at 0.00 V. Prolonged cathodic polarization gave rise to unusual behaviour, an example of which is shown in Figure 1(b) for a gold wire electrode prepolarized at −1.00 V for 30 min; other detailed discussions,

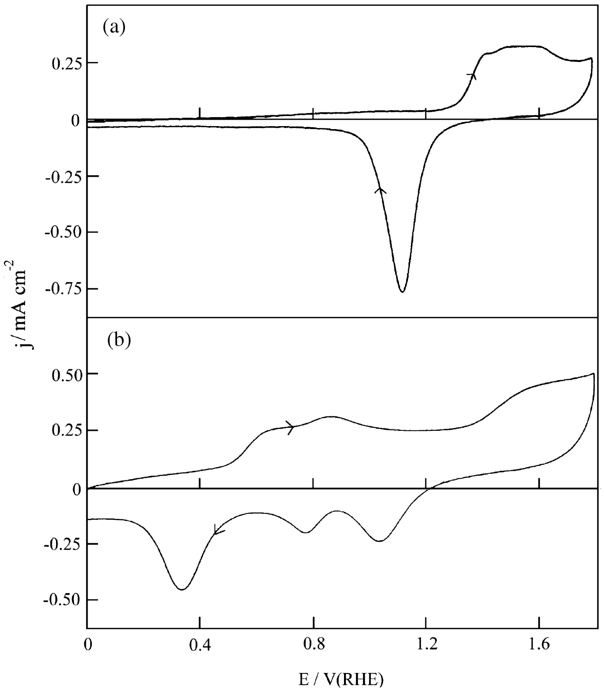

Fig. 1. Cyclic voltammograms (0.00–1.80 V, 50 mV s^{-1}) for gold in phosphate buffer solution, pH 6.9: (a) non-activated gold wire; (b) electrode prepolarized at −1.00 V for 30 min in the phosphate buffer, $T = 25$ °C.

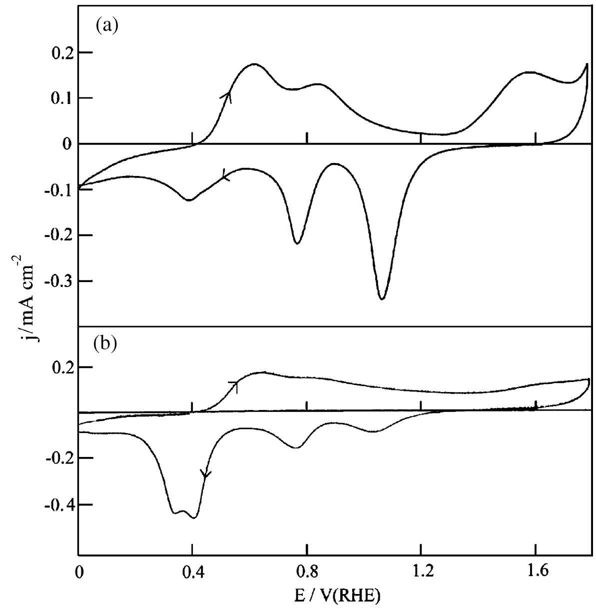

Fig. 2. Cyclic voltammogram 0.00–1.80 V, 50 mV s^{-1}) for (a) a gold wire electrode, prepolarized at −1.00 V for 30 min, followed by repetitive cycling (0.00–1.80 V, 50 mV s^{-1}) for 20 min and (b) a similar electrode previously heated in a natural gas/oxygen flame and allowed to cool rapidly in air, in a phosphate buffer solution, pH 6.9, $T = 25$ °C.

for gold in acid solution, appear in [14, 26]. In the positive sweep a steadily increasing anodic current was observed over the potential range 0.00–0.50 V; this was followed by two broad overlapping anodic peaks, at ~0.62 and 0.85 V, comparable in magnitude to the monolayer oxide formation response which began at ~1.30 V. On the subsequent negative sweep the monolayer oxide reduction response was observed over the potential range of ~1.20–0.90 V. Below this region two cathodic peaks were observed, centred at 0.76 and 0.36 V, respectively; these were followed by an envelope of cathodic current (or charge) which extended from 0.20 V to the end of the sweep at 0.00 V.

Another unusual response is shown in Figure 2(a); this voltammogram was recorded for a wire electrode which had been prepolarized at −1.00 V for 30 min followed by repetitive potential cycling (0.0–1.80 V at 50 mV s^{-1}) for 20 min. In the positive sweep cathodic current was observed initially over the range 0.00–0.40 V (such behaviour was noted earlier [14] for gold electrodes precathodized in acid solution); this was followed by two broad, overlapping, anodic peaks centred at ~0.64 and 0.85 V, respectively. A large upsurge of anodic current, corresponding to the onset of monolayer oxide film formation commenced as usual at ~1.30 V. On the subsequent negative sweep the monolayer oxide response was observed over the usual potential range 1.20–1.00 V. Below this region two rather well-defined cathodic peaks were again observed at ~0.75 and 0.38 V, respectively, followed by a cathodic response which continued over the range 0.30–0.00 V. Repetitive cycling, in addition to precathodization, had four major effects: (i) cathodic current was observed in the initial stages of the positive sweep, (ii) the anodic peaks below 0.9 V were more clearly defined, (iii) the envelope of anodic current from 0.90 to 1.30 V decreased, and (iv) the height of the first cathodic peak in the double layer region increased whereas that of the second decreased. The most interesting factor is that the active state responses are still very evident at the end of the 20 min period of repetitive cycling.

3.2. *Effect of thermal pretreatment*

An illustration of the effect of thermal pretreatment is shown in Figure 2(b). This cyclic voltammogram was recorded for a gold wire that had been strongly heated in a Bunsen flame followed by rapid cooling in air (a more detailed account of the responses of thermally pretreated Au and Pt electrodes in aqueous acid solution was given earlier [11–13]). In the positive sweep a cathodic response was observed, as in Figure 2(a), from 0.00 to 0.20 V; this was followed by an upsurge in anodic current at ~0.45 V. A steadily decreasing anodic current, apart for a slight inflection at ~0.90 V, was recorded over the range 0.60–1.40 V. This was followed by a very slight increase in anodic current over the normal monolayer oxide film formation region. In the subsequent negative sweep a surprisingly small monolayer oxide reduction response was observed at ~1.05 V; further cathodic features were observed at ~0.78 and 0.38 V, the latter (a doublet) being the major feature of the negative sweep. Comparison of the two responses for activated gold in Figure 2 shows that the general features are very similar, although the resolution and relative magnitudes of the peaks differ. In the case of the thermally pretreated gold, Figure 2(b), the active state oxidation response is greatly enhanced, at the expense of the conventional monolayer oxide feature. It is interesting that virtually the same type of response as shown here in Figure 2(b) has been reported for a thick film gold electrode, prepared by screen printing plus thermal pretreatment, by Bisenberger and coworkers (full line in Figure 3 in [25]).

3.3. *Effect of multilayer hydrous oxide growth and reduction on the response for gold*

Growing a thick hydrous oxide film followed by slow reduction of this material is another method that has been used [16] to activate a metal surface. Two hydrous oxide growth techniques [27] were employed in the present work; the first involved repetitive potential cycling (0.80–2.20 V, 50 V s^{-1} for 10 000 cycles) and

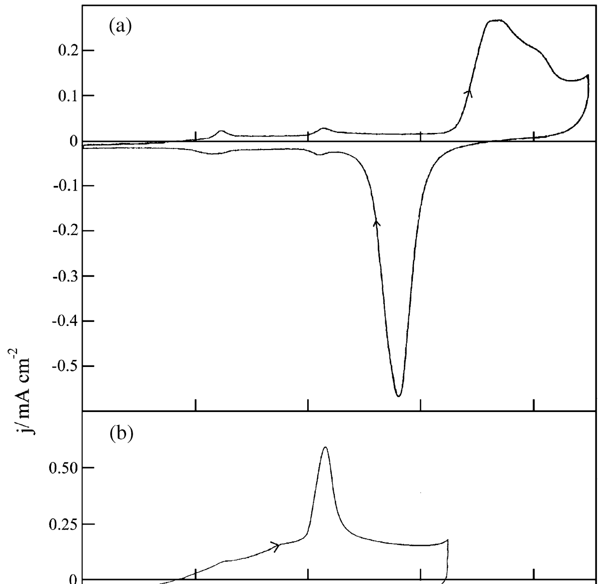

Fig. 3. Gold electrodes activated by hydrous oxide growth [27] and reduction: (a) electrode cycled, 0.80–2.20 V, 50 V s^{-1}, 10 000 cycles; the oxide film was reduced, 1.20–0.00 V, 2 mV s^{-1}, and above cyclic voltammogram then recorded (0.00–1.80 V, 50 mV s^{-1}). (b) A hydrous oxide film was grown by d.c. polarization at 2.80 V for 20 min. This film was reduced as in (a) and the above response was recorded (0.00–1.30 V, 50 mV s^{-1}). the electrolyte in all cases was phosphate buffer of pH 6.9, $T = 25$ °C.

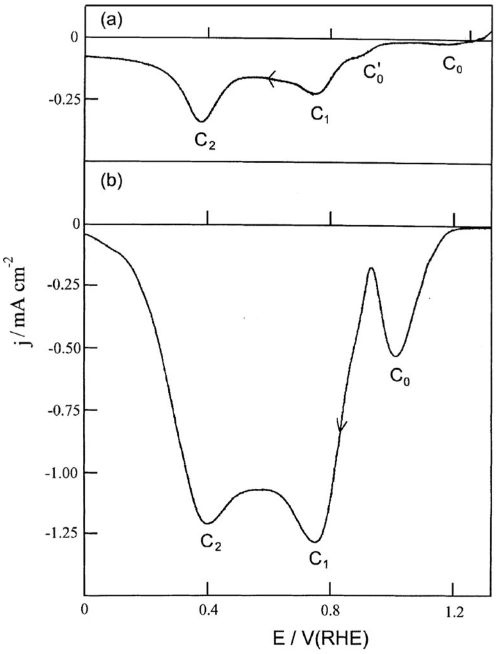

Fig. 4. Reduction profiles (1.30–0.00 V, 2 mV s^{-1}) for hydrous oxide-coated gold wire electrodes in a phosphate buffer, pH 6.9, at 25 °C; oxide film produced by potential cycling (described in Figure 3): (a) 0.80–2.40 V, 50 V s^{-1}, 5000 cycles; (b) 0.73–2.60 V, 50 V s^{-1}, 10 000 cycles.

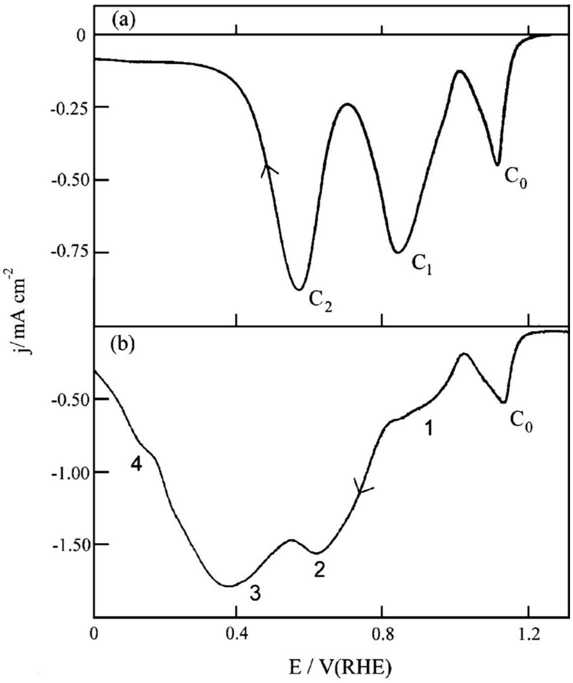

Fig. 5. Reduction profiles (1.30–0.00 V, 2 mV s^{-1}) for an oxide-coated gold wire electrode in a phosphate buffer, pH 6.9, at 25 °C. Electrode prepolarized as in Figure 3(b), at 2.8 V to produce hydrous oxide coating for (a) 3 min and (b) 20 min.

the second involved polarization of the electrode in the oxygen evolution region (2.80 V for as long as 20 min). All solutions were purged with a flow of N_2 gas prior to the slow reduction of the hydrous oxide film. The responses for the multilayer hydrous oxide reduction experiments are shown later (Figures 4 and 5); the responses shown here in Figure 3 are sweeps recorded immediately after such experiments with gold surfaces activated as a result of reduction of these thick oxide films.

The cyclic voltammogram recorded after the first oxide growth and reduction method of activation is shown in Figure 3(a). In the positive sweep small anodic peaks were observed at ~0.49 and 0.85 V. This was followed by regular monolayer oxide film formation which commenced at ~1.30 V. On the subsequent negative sweep this monolayer oxide film underwent reduction as usual over the range 1.20–1.00 V. Below this region two small cathodic peaks, at ~0.83 and 0.46 V, respectively, were observed; the premonolayer oxidation responses in this case were quite small but surprisingly reversible in character (note also the small cathodic response at the early stages of the positive sweep in Figure 3(a)).

An example of a cyclic voltammogram recorded after the second oxide growth and reduction method of activation is shown in Figure 3(b). In the positive sweep cathodic current was observed initially over the range 0.00–0.35 V. This was followed by a steadily increasing anodic current until ~0.80 V where a sharp anodic peak, with a maximum at ~0.86 V, was observed. On the subsequent negative sweep a sharp cathodic peak, evidently the counterpart of that observed on the positive sweep, was recorded at ~0.80 V. This was followed by a plateau region that extended over the range 0.70–0.40 V. A steadily decreasing cathodic current was observed until the end of the sweep at 0.00 V; the reversible transition at ~0.46 V was not well defined. The monolayer oxide formation and reduction responses, which entail the use of an upper limit above 1.30 V, are not present in Figure 3(b) as the main emphasis in the present work was on premonolayer oxidation behaviour.

3.4. *Hydrous oxide reduction responses*

Examples of cathodic responses recorded in negative sweeps following oxide growth by potential cycling are shown in Figure 4; similar data are shown in Figure 5 for films grown, for different periods of time, by d.c. polarization. The negative sweeps in these experiments began, after brief deoxygenation of the solution with N_2 gas, at 1.30 V; no oxide reduction response was observed above the latter value. The first point to note is the low level of the oxide reduction responses; much larger responses, or thicker hydrous oxide deposits, are readily produced [28] when the potential cycling technique is used in the case of gold in aqueous acid solution. It was established in preliminary experiments that varying the oxide growth conditions did not significantly increase the amount of oxide formed in neutral solution. Evidently the low activity of hydrogen and hydroxide ions, plus the adsorption of phosphate anions at the interface, adversely affect hydrous oxide growth on gold in solutions of intermediate pH values.

The first cathodic peak (C_0) in Figures 4 and 5 began at ~1.2 V and, by analogy with the response for bare gold in Figure 1, this peak is attributed to monolayer oxide film reduction. This response is quite small in the case of Figure 4(a) and such behaviour may be due to the presence of an intermediate (partially hydrated) oxide (note the presence of a second, low level shoulder, C_0', in this case). Larger cathodic peaks, one at ~0.8 V and another at ~0.4 V, attributed to hydrous oxide reduction behaviour, are evident in Figure 4. The peak resolution is poor due to the presence of a large background current over the region between these two maxima. However, it is quite interesting that the maxima for peaks C_1 and C_2 in Figure 4 coincide reasonably well with those for the cathodic peaks in the double layer region of the negative sweeps for activated gold in Figure 2. This obviously supports the earlier assumption [22, 29] that the product formed on oxidation of highly active surface metal atoms is a hydrous (or β), rather than a monolayer (or α), oxide species.

The reduction responses for oxide films growth by dc polarisation, Figure 5, were more complex. Peak C_0, attributed to monolayer oxide reduction, is evident in both cases. In Figure 5(a), where the polarization time at 2.8 V was shorter (3 min), there are two reasonably well resolved cathodic peaks at lower potentials, with maxima at ~0.84 V and ~0.56 V, respectively. The oxide reduction response below 1.0 V in Figure 5(b), where the time for polarization at 2.8 V was much larger (20 min), is much more complex; it consists of a broad envelope of cathodic charge with indications of four ill-defined maxima or points of inflection after peak C_0. Two points are worth noting about the experiments summarized in Figure 5. The potential required to grow a significant thickness of hydrous oxide film on gold in neutral solution (2.8 V) is unusually high; under constant d.c. polarization conditions such oxide growth is accompanied by quite vigorous oxygen gas evolution, probably resulting in the formation of a partially dehydrated oxide film and a significant degree of phosphate anion incorporation in the latter. Furthermore, the response shown in Figure 5(b) may be regarded as a rather extreme case as the oxide growth polarization time, at 2.8 V, extended in this case to 20 min. It is assumed here that the behaviour of hydrous oxide films on gold in solutions of neutral pH is more appropriately characterized by the data shown in Figure 4; however, some electrocatalytic reduction processes on gold (even for quite strong oxidants, see Figure 8) commenced and terminated at ~0.2 V and the only indication of an oxide/active metal redox transition in this region is peak (or shoulder) 4 in Figure 5(b).

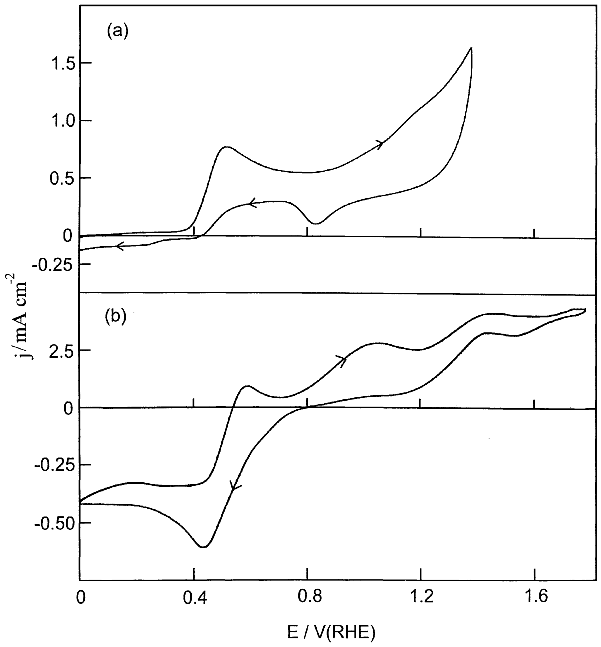

Fig. 6. Cyclic voltammogram (0.00–1.40 V, 50 mV s^{-1}) for an unactivated gold wire electrode in (a) a phosphate buffer + 0.075 mol dm^{-3} diethyl amine and (b) a phosphate buffer + 0.01 mol dm^{-3} hydrogen peroxide, $T = 25$ °C, pH 6.9.

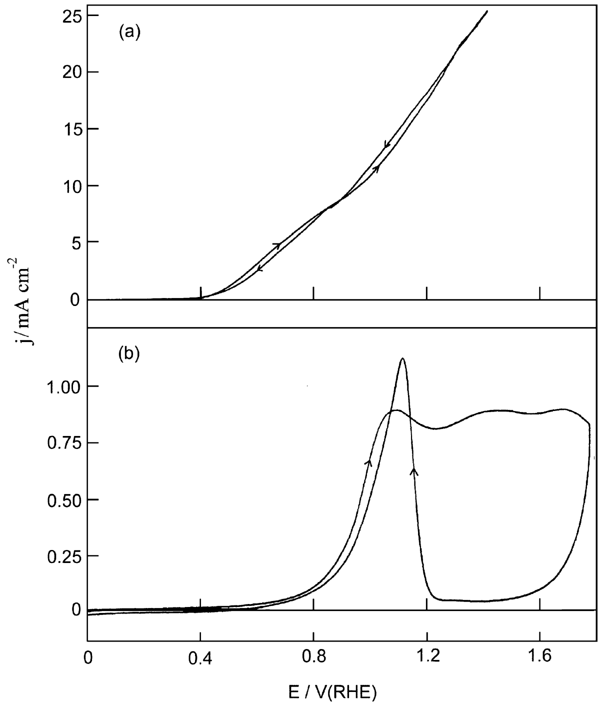

Fig. 7. Cyclic voltammogram (0.00–1.6 V, 50 mV s^{-1}) for an unactivated gold wire electrode in (a) phosphate buffer + 0.05 mol dm^{-3} hydrazine and (b) a phosphate buffer + 0.075 dm^{-3} glyoxal, $T = 25$ °C, pH 6.9.

3.5. *Electrocatalysis*

Some electrocatalytic responses observed with bare, polycrystalline gold electrodes in neutral aqueous media are shown in Figures 6–8. In the case of diethyl amine, Figure 6(a), oxidation commenced (positive sweep) and terminated (negative sweep) at ~0.4 V, that is, in the region of the first reversible premonolayer oxidation response shown for slightly activated gold in Figure 3(a). There was a second reversible redox transition

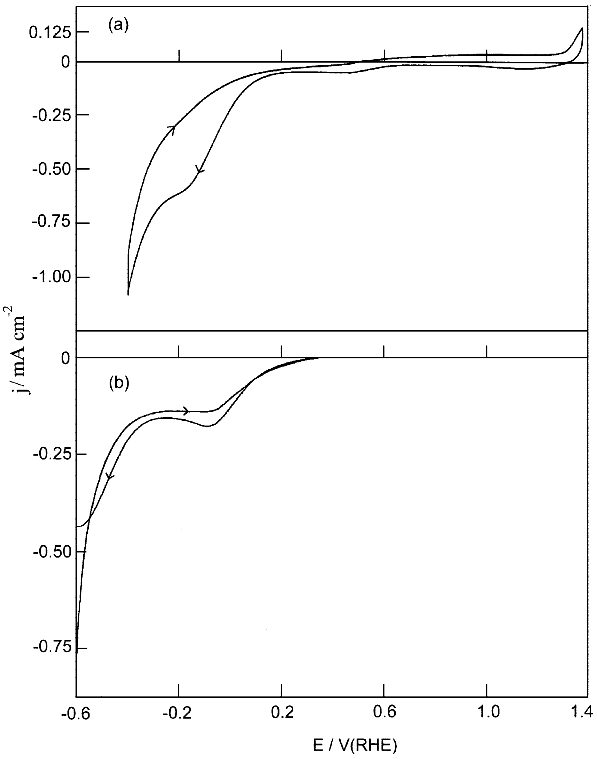

Fig. 8. Cyclic voltammogram (–0.40–1.40 V, 50 mV s^{-1}) for an unactivated gold wire electrode in (a) phosphate buffer + 0.002 mol dm^{-3} $K_2S_2O_8$ and (b) a phosphate buffer + 0.001 dm^{-3} KIO_3, $T = 25$ °C, pH 6.9.

in the latter diagram at about ~0.8 V and a corresponding increase in anodic current above this value in the positive sweep in Figure 6(a). However, in the latter diagram this second increase above 0.8 V was far less dramatic than that at ~0.4 V.

A considerably different response was observed for gold in neutral solution in the presence of hydrogen peroxide, Figure 6(b). In the positive sweep reduction occurred at virtually a potential-independent rate over the range 0.0–0.4 V; just above 0.4 V the rate of reduction decreased rapidly and this was followed by a more gradual increase in the rate of oxidation beginning just below 0.8 V; a further increase in oxidation began at ~1.2 V, that is, close to the onset of monolayer oxide formation. This drop in the rate of peroxide reduction at ~0.4 V, Figure 6(b), coincided with the increase in the rate of diethyl amine oxidation at the same potential, Figure 6(a); such a trend (for quite different reactants, and opposite types of reaction), as pointed out earlier [29], is in excellent agreement with the interfacial mediator approach to noble metal electrocatalysis. There was no cathodic response due to monolayer oxide reduction at the early stages of the negative sweep. The deposit in question is assumed to be reduced, via a local cell mechanism, by reaction with peroxide. To a large extent the changes in the negative sweep correspond to a reversal of those in the positive sweep; the main difference is that the increase in oxidation rate over the range of 0.7–1.0 V in the positive sweep has no obvious counterpart in the negative sweep.

Oxidation of hydrazine on gold in neutral solution commenced and terminated, Figure 7(a), at ~0.4 V. The maximum rate of oxidation in this case (~25 mA cm^{-2} at 1.4 V) was quite large and the responses for the positive and negative sweeps virtually overlapped. In this case there was a change in slope in the i/E response at ~0.85 V (i.e., an acceleration of the increase in the rate of hydrazine oxidation with potential occurred in the positive sweep at the latter value).

In the case of glyoxal, Figure 7(b), the rate of oxidation below 0.8 V was quite slow but as the potential increased beyond the latter value in the positive sweep a dramatic increase in rate, rising to approximately a plateau value, was observed (note the further slight increase, evident in a more marked form with peroxide, Figure 6(b), at ~1.2 V). The formation of the monolayer oxide deposit at the upper region of the positive sweep had a strongly inhibiting effect on the glyoxal oxidation rate at the beginning of the negative sweep. However, removal of this blocking film at ~1.2 V resulted in a dramatic surge in oxidation current; below 1.0 V the rate of oxidation for the positive and negative sweeps virtually coincided, the rate of oxidation decreasing rapidly, as the potential dropped, in the negative sweep at $E <$ ~1.0 V.

The dramatic difference in anodic current densities attained with hydrazine and glyoxal, Figure 7, cannot be completely explained at the present time. Hydrazine is a small molecule with strong reducing properties; it may be capable of penetrating the hydration sphere of the gold oxide mediator species at surface active sites and, therefore, undergo rapid reaction via an inner-sphere reaction mechanism. The reaction products, N_2 and H_2O, are unlikely to inhibit the reaction of further hydrazine molecules at such sites. Aldehyde oxidations occur through intermediate 1,1 diols or hydrates [30], formed by reversible nucleophilic addition of water to the carbonyl group, namely,

$$\mathrm{RCHO} + \mathrm{H_2O} = \mathrm{RC(OH)_2} \qquad (1)$$

The equilibrium for the above reaction lies to the left and hence the concentration of the diol present is usually quite low and its oxidation may occur via an outer-sphere mechanism. The oxidation product at pH 7 is assumed to be a carboxylate anion ($RCOO^-$) which may well be slow to leave the cationic (Au^{3+}) mediator centre. Thus, there may be a number of factors contributing to the sluggish oxidation behaviour of the glyoxal at the gold anode.

Two further electrocatalytic responses, for persulphate (a) and iodate (b) reduction on gold in phosphate buffer solution, are shown in Figure 8. Very little sign of reduction was observed with these two compounds, which are rather strong oxidants, above 0.2 V. The only oxide film response observed at the latter potential for gold in solutions of neutral pH is peak (or shoulder) 4 in Figure 5(b).

3.6. *Observation of electrocatalytic behaviour with gold in acid solution*

Premonolayer oxidation behaviour of noble metals, that is, oxidation of metal electrode surfaces in aqueous media at potentials that are well within the conventional double layer region, was initially a controversial topic [31]. However, recent independent investigations, of both silver [17–20] and copper [32] in base, involving the use of sophisticated surface analytical techniques, have confirmed the formation of oxyspecies at the interface within the double layer region. Whether the interfacial reaction in question should be regarded as a hydroxide adsorption or metal hydroxide formation process is largely a matter of semantics. However, it is interesting to note that in describing SERS data for premonolayer oxidation of silver in base Doblhofer and coworkers [17] attributed the spectroscopic responses to the stretching and bending of bonds in a surface metal hydroxide, AgOH, species. We also favour this metal hydroxide viewpoint as quite often multilayer hydrous oxide reduction responses (which are obviously not due to adsorbed species) coincide quite well, in terms of potential values, with premonolayer oxidation and electrocatalytic behaviour. This was demonstrated here for gold and earlier for both copper in base [29] and platinum in acid solution [31].

There was a tendency previously (e.g., in the case of gold [33]) to dismiss premonolayer oxidation responses as being due to the involvement of impurities. To some extent this is understandable, for example, for gold in acid solution large anodic peaks below 0.6 V in the positive sweep, Figure 9(a), recorded after thermal [13] or cathodic [14] activation, appear to be anodic stripping peaks of the type expected for a low coverage of a metal impurity (e.g., copper). The presence of two anodic peaks below 0.6 V in this case suggest the involvement of two impurity species.

It is important to note that with regard to anodic behaviour the superactive state of gold has characteristics which, like an impurity such as copper, are different from those of a stable gold surface. It is well established from metal microcluster studies [34] that, due to their low lattice stabilization energy and/or the presence of quantum confinement effects, minute metal clusters are prone to oxidation at much lower potentials than similar atoms present in the stable metal surface. Hence, it is assumed that the anodic responses below 0.6 V in Figure 9(a) are due to the oxidation of slightly different types of mobile gold adatoms or microclusters. Precise interpretation of the peak maximum potentials in terms of surface active state behaviour is not possible as the nature of both the reduced and oxidized forms of the couples involved in the interfacial redox transitions are presently uncertain.

Support for the assumption that the responses observed below 0.6 V in Figure 9 (a) are due to the redox transition of active gold, rather than impurity species, is provided by the data shown in Figure 9(b). As discussed earlier [21, 29] the interfacial redox couple, Au*/Au(OH)$_x$, is assumed to participate in electrocatalytic processes, the oxidized state, Au(OH)$_x$, being the mediator for oxidation (of dissolved solution species) while the reduced form (Au*) often functions as the mediator for reduction. The reduction response in the negative sweep for the diazo compound Janus Green B (an additive used in Damascene copper plating baths [35]) at gold in acid solution, Figure 9(b), is especially interesting. Two regions of significant increase in cathodic current, again suggesting the involvement of two distinguishable mediators, one commencing at ~0.55 V and the other at ~0.45 V, are evident. As shown by the dashed lines in Figure 9, the onset potentials for reduction in Figure 9(b) are in excellent agreement with the peak maximum potentials (E_p values) for the two active state anodic responses in Figure 9(a). It is important to note that the two gold surfaces involved in Figure 9 are quite different. The one used in Figure 9(a) was highly activated to give enhanced active state, or electrocatalytic mediator, responses. The one that gave the response shown in Figure 9(b) was a conventional unactivated gold surface. However, the coincidences, indicated here by the dashed lines in Figure 9, suggest that very similar active gold atom states exist on both surfaces, evidently as very low

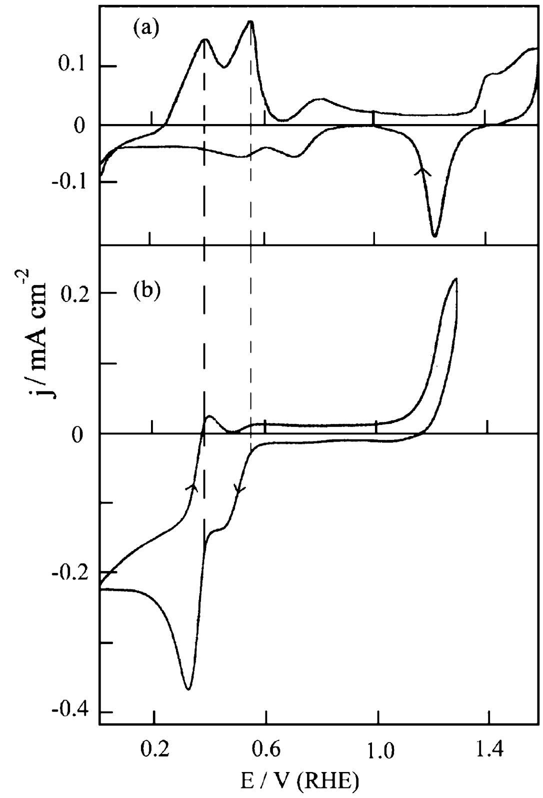

Fig. 9. (a) Cyclic voltammogram (0.00–1.6 V, 50 mV s^{-1}) for an activated gold wire electrode, thermally pretreated [13] at 905 °C for 20 s in an argon atmosphere, in 1.0 mol dm^{-3} H_2SO_4 at 18 °C; (b) cyclic voltammogram (0.00–1.3, 50 mV s^{-1}) for an unactivated gold wire electrode (as used in the present work) in 1.0 mol dm^{-3} H_2SO_4 + 0.001 mol dm^{-3} Janus Green B at 60 °C (temperature raised to accentuate response).

coverage active site species in the case of conventional gold. The existence of 'invisible' (difficult to image by scanning probe microscopy) mobile surface metal adatoms was discussed recently by Kornyshev and Sumetskii [36]. The assumption in the present work is that such atoms are often the basis of active site behaviour, especially where interfacial cyclic redox mediator electrocatalysis is involved.

The other intriguing feature in Figure 9(b) is the upsurge of anodic current in the positive sweep commencing at ~1.1 V. This is prior to the onset of monolayer oxide formation, which usually occurs at ~1.36 V vs RHE for gold in acid. This marked current increase just above 1.1 V is assumed to involve mediated oxidation of Janus Green B; again the presence of an oxide mediator system, involving an interfacial redox transition at ~1.05 V, was discussed earlier [21] for this electrode system.

4. Discussion

4.1. *Interfacial redox couples in electrocatalysis*

Premonolayer oxidation of metals is a topic of increasing interest in electrochemistry. This phenomenon was extensively investigated recently by Doblhofer and coworkers [17–20] in the case of silver in base and work of a similar nature has just been reported by Strehblow and coworkers [32] in the case of copper in base. The presence of oxyspecies at the interface at potentials well within the double layer region was considered by both groups largely in terms of adsorption, that is, formation of OH_{ads}, O_{ads} and O_{sub} (subsurface oxygen). However, it is worth noting that in interpreting SERS data for silver in base [17] Doblhofer and coworkers attributed the two observed Raman bands to 'Ag–OH stretching and AgO–H bending vibrations', that is, the Raman responses were interpreted in terms of interfacial metal hydroxide formation at low potentials. It is interesting also that in discussing the premonolayer oxidation of copper, Strehblow and coworkers represented the product of the reaction (Equation 1 in [32]) as $Cu–OH_{ads}$. The hydroxyl radical is an unusually high energy species, E° (H_2O/OH) = 2.85 V vs RHE [37]; the active surface metal atom is the species at the interface that is most likely to undergo oxidation, yielding a dipolar metal hydroxyl compound as follows:

$$M^* \xrightarrow{-e^-} M^+ \xrightarrow{H_2O} M^+\text{—}OH^- + H^+ \tag{2}$$

More than one hydroxyl group may be coordinated in some instances, for example, in the case of $Au(OH)_3$ formation; direct evidence for hydroxyl involvement in the case of premonolayer oxidation of gold in aqueous media was obtained earlier by Desilvestro and Weaver [38]. Metal hydroxide formation is a basic assumption [21, 29] in the incipient hydrous oxide/adatom mediator (IHOAM) mechanism of electrocatalysis. In a recent account of the active state and electrocatalytic behaviour of copper in base [39] a remarkable correlation (in terms of premonolayer oxidation potentials) between such behaviour and multilayer hydrous oxide film reduction was clearly demonstrated. A similar correlation is evident in the present work with gold in neutral aqueous media.

According to the data shown in Figure 4 multilayer hydrous oxide films (produced by potential cycling) on gold in neutral solution exhibit major reduction responses (or peaks) at ~0.8 and ~0.4 V. These are abnormally low potentials for such a reaction; thermodynamic data [40] indicates that oxide reduction on gold in aqueous media should occur at ~1.4 V and indeed the monolayer oxide film, Figure 1(a), undergoes reduction above 1.0 V. The low values for reduction of the hydrous oxide may be attributed to two factors: (i) hydrous oxides in general are low density materials [27]; the basic unit is assumed to be a dimeric species, $Au_2O_3 \cdot nH_2O$ (the precise nature of the oxide will not be discussed here). Reduction of these species is assumed to involve initial formation of virtually discrete, poorly lattice stabilized surface gold atoms; such a reaction route, involving a high energy intermediate, entails a significant negative shift in the oxide reduction potential. (ii) The second source of complexity is the hydrous oxide species. It should be borne in mind that apparently simple oxides, such as MnO_2, are almost infinitely variable in structure [41]. Such structural diversity is due to different packing arrangements of the basic octahedral units in the solid; planes, rings, regular and irregular vacancies may be present. With hydrous gold; oxide films the unsintered deposits may be structurally heterogeneous and the density may not be uniform. In addition, there may be local variations in water, anion or cation content. Such variation of the oxidized state of the interfacial couple is assumed to significantly affect the β oxide reduction potential.

The appearance of two, Figure 3(a), and possibly more, Figure 5(b), hydrous oxide/metal transitions in the case of gold in neutral solution cannot be explained explicitly at the present time. Such behaviour is apparently not unusual as a similar type of diversity was reported recently for platinum in aqueous acid solution [42]. There is obviously much scope for further work, both at a practical and theoretical level, on the behaviour of highly active states of metal electrode surfaces. The difference in redox potentials (0.45 and 0.85 V) in the present case correspond essentially to the reaction of different couples. The reduced state, gold atoms, are nominally identical but may differ significantly in activity due to variation in lattice stabilization energy. Similarly the oxidized states, the hydrous oxide species, may differ in structure, and composition. These two states of the couple are assumed to be interrelated, that is, the nature of the oxide may influence the level of activity of the atom formed on reduction and a similar effect may arise in the course of oxidation. From both an experimental and theoretical viewpoint, the fact that both transitions involve the reaction of unstable states is a major complication.

The agreement, in terms of potential values, between the premonolayer oxidation responses, Figure 3(a), and the electrocatalytic behaviour, Figures 6 and 7, is also in accordance with the IHOAM theory of electrocatalysis [29]. In the positive sweep the more active surface gold atoms undergo oxidation at ~0.4 V; such a process has two effects from an electrocatalytic viewpoint: (i) it provides the oxide mediator, or oxidant, $[Au_2O_3 \cdot nH_2O]_{ads}$, for the oxidation of such species as diethyl amine, Figure 6(a), and hydrazine, Figure 7(a) (in both cases the anodic current in the positive sweep increased rapidly at ~0.4 V); and (ii) it removes the adatom mediator (or reductant, Au_{ads}) for the reduction of species such as hydrogen peroxide; Figure 6(b); (note the rapid drop in cathodic current in the positive sweep at ~0.4 V).

Low level faradaic responses within the double layer region in the case of noble metal electrodes tend to be attributed to impurity effects. This may be valid in some cases but is evidently not invariably correct. There is now widespread evidence in the case of gold [38, 43], silver [17–20] and copper [32] electrodes in base with regard to the formation of premonolayer oxyspecies. Also, the transition at ~0.4 V for gold in neutral solution correlates well with multilayer hydrous oxide reduction, Figure 4, activated metal oxidation, Figure 2, and electrocatalytic responses, Figure 6. An impurity is likely to deactivate a surface; however, with the electrode of interest here the surface is active with regard to the electrocatalysis both above and below the critical potential value of ~0.45 V; the IHOAM model provides a logical account of such behaviour.

The species involved in the redox transitions at ~0.4 and 0.8 V (Figure 3(a)) do not exist in isolation. There are other species (e.g., phosphate anions) present at the interface, possibly attached to the gold surface. The presence of such anions is assumed to severely inhibit hydrous oxide growth on gold in neutral media. The complex oxide reduction response shown in Figure 5(b) is assumed to reflect the effect of anion inhibition of the oxide growth reaction, plus the effect of the prolonged severe anodization on the nature and reactivity of the film. There is an additional source of complication in the case of electrocatalytic reactions since the solution reactant must now react directly with either the reduced or oxidized form of the interfacial couple. This may result in the solution reagent influencing the nature of the mediator system, for example, the structure of the oxide and the potential at which it reacts. For example, in the case of persulfate and iodate reduction (Figure 8) the interfacial hydrous oxide species is produced, in terms of the IHOAM approach, by reaction of these dissolved oxidants with active surface gold atoms. If the hydrous oxyspecies produced in such reactions is unusual, then it may not be too surprising that the mediator transition potential, and the onset of electrocatalysis, is shifted, as observed, Figure 8, to unexpected values. The expected values, in the present case, on the basis of the data in Figure 3(a), are ~0.4 and 0.8 V. Another example of a response at an unusual potential, at ~1.2 V, is evident in the case of peroxide oxidation, Figure 6(b); in this case the peroxide is assumed to be oxidized via reaction with the oxidized state of the interfacial couple. A rather low energy state of the surface gold atoms is assumed to be involved in this case.

4.2. *Inadvertent production of the high coverages of the active state*

Surface active sites are intrinsically unstable, that is, they, and the associated premonolayer oxidation responses, should decay and eventually disappear with time. In practice the situation is usually more complex; for example, it was generally found that having activated a gold electrode by cathodization or thermal pretreatment (Figure 2) it was quite difficult to get the surface back to the state giving the conventional response (Figure 1(a)), that is, low level traces of the active state behaviour were usually found to be rather persistent.

It is also evident that the attainment of the active state of a metal surface does not invariably require a deliberate 'energy insertion' step, that is, a cathodization or thermal pretreatment step. Surface activation may arise inadvertently in conjunction with a surface pretreatment or preparation step. This topic is of significant interest at the present time in the microchip metallization area where copper films, produced by electrodeposition, are usually found to be in an active, poorly ordered, state [3].

There are at least two earlier reports of what appear to be premonolayer oxidation responses for gold in neutral aqueous media. Both attributed the responses, which occurred within the double layer region, to the presence of impurities; however, in view of what is now known concerning the behaviour of active gold, such an interpretation may not be valid. Craston and coworkers [24] prepared microband electrodes by heating screen-printed patterned coatings of gold inks, or powders, on alumina tiles at about 850 °C for 15 min. This may be regarded as thermal activation which, as demonstrated here, Figure 2(b), and elsewhere [13], is likely to promote active surface state and premonolayer oxidation responses. The initial scan for such a thermally prepared electrode in phosphate buffer solution (pH 7.4) showed a major quasi-reversible transition within the double layer region (Figure 4(a) in [24]). Although the involvement of impurities cannot be discounted, it seems highly likely that the same type of behaviour as mentioned here for electrodeposited copper [3] and heated gold (Figure 2(b)) also arises in the case of these thermally treated, thin gold film electrodes (since the states of the metal and the pretreatment conditions are usually different, the active state responses are rarely identical).

Cyclic voltammograms for thick-film gold sensor electrodes, also produced by thermal pretreatment of a gold ink, in 0.1 mol dm^{-3} sodium phosphate solution have been reported by Bisenberger and coworkers [25]. The response for the bare gold film (full line in Figure 3 of [25]) showed two quasi-reversible major responses within the double layer region, with little indication of the α oxide response in the positive sweep, quite like the response shown here for thermally activated gold in Figure 2(b). Obviously premonolayer oxidation behaviour may well have been the origin of such unusual sensor responses.

4.3. *Correlation of highly active state and electrocatalytic behaviour for gold surfaces in acid solution*

The complexity of gold electrochemistry, from an electrocatalytic viewpoint, is demonstrated by the behaviour indicated in Figure 9. It is generally assumed that gold in aqueous media exhibits no faradaic response in the double layer region; however, as demonstrated recently [13] major voltammetric responses are observed in the positive sweep when thermally activated gold electrodes are immersed in acid solution, Figure 9(a). Details of such behaviour were discussed in the earlier report; the lack of reversible redox peak behaviour in the region below 0.6 V in the latter diagram was attributed to partial loss of contact between the hydrous oxide species and the electrode surface. It is assumed that such contact problems do not arise at low coverage active sites (see the much more reversible behaviour in the double layer region in Figure 3(a)).

A remarkable feature of the data in Figure 9 is the correlation between the highly active gold surface undergoing premonolayer oxidation below 0.6 V in (a) and the electrocatalytic reduction responses at a conventional, unactivated gold wire (see the negative sweep in Figure 9(b)) with Janus Green B present in the solution. Such behaviour is in excellent agreement with the IHOAM view of electrocatalysis and strongly supports the superactive state view of metal surface behaviour. The anodic oxidation response just above 1.10 V in Figure 9(b) is also in agreement with an earlier account of the electrocatalytic properties of gold in acid solution [21]. It was postulated that there was an interfacial mediator in this region which is active with respect to oxidation of compounds such as glycerol, benzyl alcohol, tartonic and mesooxalic acid and cystine at gold in acid solution.

The IHOAM model of electrocatalysis has been applied to a number of metals and is in agreement with Taylor's original proposal that low coverage active surface sites are involved, and that the vital ingredient at such sites are low coordination, highly active metal atoms. The approach explains why in many cases electrocatalysis is often confined to the double layer region, this being the region where active metal atoms undergo redox transitions. From a fundamental viewpoint this approach raises some interesting questions, for example, what determines the mediator transition potentials or can the observed values, at 0.45 and 0.85 V in Figure 3(a), be predicted? A degree of caution is probably required when extending the IHOAM approach to strongly chemisorbing metals such as platinum. With the latter metal activated chemisorption usually involves electron donation from the chemisorbing molecule to in the d-band of the metal, that is, extended bulk properties (modified by structural defects) are important. However, localized adatom behaviour (as typified by the IHOAM approach) may also be relevant, i.e. there may well be a dual mechanism for electrocatalysis with some metals, with one or other predominating, depending largely on the reaction being catalysed. For instance in the case of H_2 oxidation on Pt the activated chemisorption route is assumed to predominate; however, in the case of CO_{ads} oxidation on Pt in aqueous acid media the IHOAM route is probably vital, the incipient oxide providing the oxygen required to convert the CO_{ads} to CO_2.

From a general viewpoint there are some intriguing features in the active site, or superactive state, approach to metal surface behaviour. For example, with unactivated gold (Figure 1(a)) there is scarcely a hint of an active state response; yet such a state, or states, must either exist or be capable of facile generation as this is the type of unactivated surface that gives rise to dimethyl amine oxidation above, and peroxide reduction below, ~0.4 V, (Figure 6). The vital ingredient in active state behaviour may well be a transient species, of quite low mean coverage; for example, adatoms migrating between different kink or ledge sites. Enhanced double layer responses, as in Figure 2, are assumed to reflect increased coverages of adatoms associated with greater coverages of gross defects on vigorously perturbed, superactivated surfaces.

Not only is the superactive surface state coverage normally low (about 2% of a monolayer) but in some cases [21, 42] there seems to be a further subdivision into about four different active state or mediator responses; it is not clear at this stage what constitutes, or differentiates between, these substates, or if they are totally independent. Electrochemical techniques (e.g., cyclic voltammetry) seem to be the only approach to date highlighting this diversity of premonolayer oxidation responses, in other words capable of clearly resolving active site responses, as illustrated by the small reversible peaks in Figure 3(a), at ~0.45 and 0.85 V.

Finally, the involvement of active, or labile, states of metal surfaces in electrocatalytic processes is in agreement with the ideas of the chemistry Nobel Laureate, Barry Sharpless [44], who has pointed out the limitations of a structural approach in catalysis. The observed structure relates to the resting state of the catalyst: when the catalyst is participating in a reaction, movement is involved. Such movement, lack of rigidity and unusual reactivity of active metal atoms is a vital factor in electrocatalysis at surfaces.

5. Conclusions

(i) Active, metastable states are well known for bulk metals and confer unique and commercially valuable properties on the latter. Such states also arise in the case of metal surfaces and affect the voltammetric behaviour of the latter. In view of recent independent work, involving considerable use of nonelectrochemical techniques [17–20, 38], there can be little doubt as to the reality of premonolayer oxidation at metal/aqueous solution interfaces.

(ii) Metastable surface states are difficult to investigate as they are not easily produced in a highly reproducible form and are prone to alter with time and treatment. Also, such states may not be very amenable to detailed investigation by high resolution surface microscopy techniques as they are often quite rough and disordered [13, 26] and, more importantly, highly active entities present (e.g., adatoms) are mobile species and this, according to Kolb [6], provides imaging problems in the case of STM.

(iii) Cyclic voltammetry provides useful data on premonolayer behaviour, for example, to demonstrate the presence of more than one active state interfacial transition (Figure 3(a)). It also provided much of the early evidence for premonolayer oxidation in the case of many metal electrode systems, including silver in base [45]. In the present work it was demonstrated, for the first time in the case of gold in neutral solution, that premonolayer oxidation, multilayer hydrous oxide reduction and the onset/termination behaviour of electrocatalytic reactions often correlate with IHOAM theory [29] in terms of potential values. The present work supports the assumption that active surface state behaviour, although complex, is nevertheless an important area of research which merits detailed investigation.

(iv) The present data on the behaviour of gold in neutral aqueous media is of relevance in the study of amperometric microsensors and biosensors [25] for not only does it show how some of these sensors operate, but also it emphasizes the need for caution in the case of the gold deposition and pretreatment steps. Extensive coverage of the superactive surface state should be avoided.

References

1. C. Suryanarayana, *in* R.W. Cahn, P. Haasen and E.J. Kramer (Eds), 'Materials Science and Technology', Vol. 15 (VCH, Weinheim, 1991), pp. 59–110.
2. R.E. Reed-Hill and R. Abbaschian, 'Physical Metallurgy Principles', 3rd edn (PWS-Kent, Boston, 1992), pp. 227–242.
3. P.C. Andricacos, *Electrochem. Soc. Interface* **8** (1999) 32.
4. J.M.E. Harper and K.D. Rodbell, *J. Vac. Sci. Technol. B* **15** (1997) 763.
5. A.W. Adamson, 'Physical Chemistry of Surfaces', 3rd edn, (J. Wiley & sons, New York, 1976), p. 244.
6. D.M. Kolb and M.A. Schneeweiss, *Electrochem. Soc. Interface* **8** (1999) 26.
7. L.A. Kibler, A. Cuesta, M. Kleinert and D.M. Kolb, *J. Electroanal. Chem.* **484** (2000) 73.
8. G.A. Somorjai, *Chem. Rev.* **96** (1996) 1223.
9. H.S. Taylor, *Proc. R. Soc. Lond. A* **108** (1925) 105.
10. L.D. Burke, J.K. Casey and J.A. Morrissey, *Electrochim. Acta* **38** (1993) 897.
11. L.D. Burke and L.M. Hurley, *Electrochim. Acta* **44** (1999) 3451.
12. L.D. Burke and L.M. Hurley, *J. Solid State Electrochem.* **4** (2000) 353.
13. L.D. Burke, L.M. Hurley, V.E. Lodge and M.B. Mooney, *J. Solid State Electrochem.* **5** (2001) 250.
14. L.D. Burke and A.P. O' Mullane, *J. Solid State Electrochem.* **4** (2000) 285.
15. L.D. Burke, J.A. Collins, M.A. Horgan, L.M. Hurley and A.P. O'Mullane, *Electrochim. Acta* **45** (2000) 4127.
16. L.D. Burke and L.C. Nagle, *J. Electroanal. Chem.* **461** (1999) 52.
17. E.R. Savinova, P. Kraft, B. Pettinger and K. Doblhofer, *J. Electroanal. Chem.* **430** (1997) 47.
18. D.Y. Zemlyanov, E.R. Savinova, A. Scheybal, K. Doblhofer and R. Schlögl, *Surf. Sci.* **418** (1998) 441.
19. Sh.K. Shaikhutdinov, E.R. Savinova, A. Scheybal, K. Doblhofer and R. Schlögl, *J. Electroanal. Chem.* **500** (2001) 208.
20. E.R. Savinova, D. Zemlyanov, B. Pettinger, A. Scheybal, R. Schlögl and K. Doblhofer, *Electrochim. Acta* **46** (2000) 175.
21. L.D. Burke and P.F. Nugent, *Gold Bull.* **31** (1998) 39.
22. L.D. Burke, A.J. Ahern and A.P. O'Mullane, *Gold Bull.* **35** (2002) 3.
23. D.C. Johnson and W.R. LaCourse, *Anal. Chem.* **62** (1990) 589A.
24. D.H. Craston, C.P. Jones, D.E. Williams and N. El Murr, *Talanta* **38** (1991) 17.
25. M. Bisenberger, C. Bräuchle and N. Hampp, *Sens. Actuators B* **28** (1995) 181.
26. L.D. Burke, A.P. O'Mullane, V.E. Lodge and M.B. Mooney, *J. Solid State Electrochem.* **5** (2001) 319.
27. L.D. Burke and M.E.G. Lyons, *in* R.E. White, J.O'M. Bockris and B.E. Conway (Eds), 'Modern Aspects of Electrochemistry', No. 18 (Plenum, New York, 1986), pp. 169–248.
28. L.D. Burke and P.F. Nugent, *J. Electroanal. Chem.* **444** (1998) 19.
29. L.D. Burke, J.A. Collins and M.A. Murphy, *J. Solid State Electrochem.* **4** (1999) 34.
30. J. McMurray, 'Organic Chemistry' (Brooks/Cole, New York, 5th edn, 2000) p. 760.
31. L.D. Burke, *Electrochim. Acta* **39** (1994) 1841.
32. H.-H. Strehblow, V. Maurice and P. Marcus, *Electrochim. Acta* **46** (2001) 3755.
33. R. Woods, *in* A.J. Bard (Ed.), 'Electroanalytical Chemistry', Vol. 9 (Dekker, New York, 1976), p. 119.
34. A. Henglein, *Ber. Bunsenges. Phys. Chem.* **99** (1995) 903.
35. P. Taiphaisitpongs, Y. Cao and A.C. West, *J. Electrochem. Soc.* **148** (2001) C492.
36. A.A. Kornyshev and M. Sumetskii, *in* W.J. Lorenz and W. Plieth (Eds), 'Electrochemical Nanotechnology' (Wiley–VCH, New York, 1998), pp. 45–55.
37. G. Milazzo and S. Caroli, 'Tables of Standard Electrode Potentials' (J. Wiley & sons, Chichester, UK, 1978), p. 229.
38. J. Desilvestro and M.J. Weaver, *J. Electroanal. Chem.* **209** (1986) 377.
39. L.D. Burke and M.A. Murphy, *J. Solid State Electrochem.* **5** (2000) 43.
40. M. Pourbaix, *in* 'Atlas of Electrochemical Equilibria in Aqueous Solutions' (Pergamon, Oxford, 1966).
41. R.G. Burns and V.M. Burns, *in* A. Kozawa and R.J. Brodd (Eds), 'Manganese Dioxide Symposium', Vol. 1, Cleveland 1975 (I.C. Sample Office, c/o Union Carbide Corporation, Parma Technical Center, PO Box 6116, Cleveland, Ohio), pp. 306–327.
42. L.D. Burke and A.J. Ahern, *J. Solid State Electrochem.* **5** (2001) 553.
43. L.D. Burke and P.F. Nugent, *Gold Bull.* **30** (1997) 903.
44. C. O'Driscoll, *Chem. Brit.* (Nov. 2001) 26.
45. L.D. Burke and W.A. O'Leary, *J. Electrochem. Soc.* **135** (1988) 1965.